

See discussions, stats, and author profiles for this publication at: <https://www.researchgate.net/publication/24262127>

Synthesis and Characterization of Glycerol Dendrons, Self-Assembled Monolayers on Gold: A Detailed Study of Their Protein Resistance

ARTICLE in BIOMACROMOLECULES · MAY 2009

Impact Factor: 5.75 · DOI: 10.1021/bm801093t · Source: PubMed

CITATIONS

74

READS

45

2 AUTHORS, INCLUDING:



Monika Wyszogrodzka

Freie Universität Berlin

10 PUBLICATIONS 306 CITATIONS

SEE PROFILE

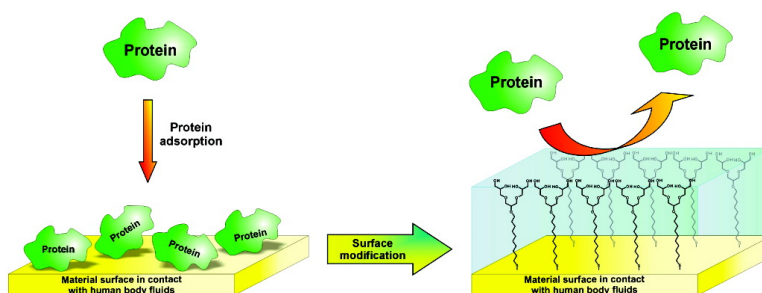
Article

Synthesis and Characterization of Glycerol Dendrons, Self-Assembled Monolayers on Gold: A Detailed Study of Their Protein Resistance

Monika Wyszogrodzka, and Rainer Haag

Biomacromolecules, 2009, 10 (5), 1043-1054 • Publication Date (Web): 07 April 2009

Downloaded from <http://pubs.acs.org> on May 12, 2009



More About This Article

Additional resources and features associated with this article are available within the HTML version:

- Supporting Information
- Access to high resolution figures
- Links to articles and content related to this article
- Copyright permission to reproduce figures and/or text from this article

[View the Full Text HTML](#)

Synthesis and Characterization of Glycerol Dendrons, Self-Assembled Monolayers on Gold: A Detailed Study of Their Protein Resistance

Monika Wyszogrodzka^{*,†,‡} and Rainer Haag[†]

*Institut für Chemie und Biochemie, Freie Universität Berlin, Takustr. 3, 14195 Berlin, Germany, and
Organische Chemie, Technische Universität Dortmund, Otto-Hahn-Str. 6, 44225 Dortmund, Germany*

Received September 26, 2008; Revised Manuscript Received February 25, 2009

Nonfouling surface coatings are of great interest for the development of advanced biomaterials used in biomedical and marine applications. Therefore, a lot of effort has been made to design new biocompatible materials and to understand the mechanisms of the protein repulsion. This study examines a series of polyglycerol (PG) dendrons modified by alkanethiols for their interactions with biofouling relevant proteins: fibrinogen (Fib), lysozyme (Lys), albumin (Alb), and pepsin (Pep). All polyglycerol dendrons [G1.0]–[G3.0] self-assembled monolayers with different terminal functionality (–OH, –OCH₃) were prepared by applying simple Williamson ether formation followed by radical thiol addition to the alkene. Surface modification was performed by chemisorption of the different dendritic PG derivatives onto gold chips from ethanolic solution and then directly used in a screening with the respective proteins applying SPR spectroscopy. The effective and time-dependent SAM formation on gold was also revealed by X-ray photoelectron spectroscopy. It was demonstrated that the all polyglycerol dendrons [G1.0]–[G3.0] possess excellent resistance to the test proteins. Surprisingly, the SAMs of easily accessible [G1.0] dendron ($M_w = 426$ g/mol) modified alkanethiol show the same high protein resistance as we could achieved for high molecular weight polymers (e.g., hyperbranched PG with $M_n = 2500$ g/mol). However, significant changes in the amount of adsorbed proteins within the studied time frame of 24 h was not observed. Therefore, these oligoglycerol dendrons are a good alternative for the commonly used poly(ethylene glycol) (PEG).

Introduction

A major problem of currently implanted and blood-contact biomaterials is the triggering of a wide variety of unwanted responses, including inflammation, infection, thrombosis, fibrosis, allergy, and biomaterial induced cancer.^{1–4} Given the inert and nontoxic nature of these materials, it is not clear how the host detects and then responds to the presence of foreign biomaterial implants. However, it is already widely accepted that these adverse responses are associated with the rapid accumulation (within a time frame of a few seconds to minutes) of a large number of blood plasma proteins long before the arrival of inflammatory cells. Further cell and bacteria adhesion, followed by Biofilm formation can lead to the significant decrease of the proper function of implants, such as heart valve replacement, catheters, or artificial organs.^{1,3} Therefore, the phenomenon of protein adsorption has attracted much attention in both academic and industrial communities for many years. To reduce these unwanted responses, the materials must be modified with an appropriate surface coating to become more resistant to proteins.

A lot of attention has been directed toward the development of chemical strategies for modifying material surfaces to lower their protein adsorption. However, biomaterials with completely inert surfaces (a surface to which no protein adsorbs) do not exist yet and are not likely to be achieved in the near future.^{1,5,6} Several materials that exhibit a significant reduction in nonspecific adsorption of proteins,⁷ like dextran,^{8–10} glycoderivates,^{11–15}

polyoxazolines,¹⁶ and zwitterionic self-assembled monolayers (SAMs), as well as polymers,^{17–19} have been identified. However, SAMs presenting poly(ethylene glycol) (PEG) groups are the most prominent and commercially available material used to repel proteins.^{20–22} Thin layers of PEG ($n \geq 3$) were already recognized in the early 90s to provide excellent resistance against circulating proteins from biological media.^{20,21} Besides the fact that PEG is nontoxic and nonimmunogenic,²³ it exhibits thermal instability²⁴ and sensitivity toward oxidation, especially under physiological conditions.^{25–27} Due to the above-described disadvantages of PEG the need for alternative materials with higher stability is still of great importance.

Even though proteins tend to adsorb more willingly to hydrophobic surfaces through hydrophobic interactions, there are many other factors than the van der Waals forces, like electrostatic and steric forces, pH, and isoelectric point, that strongly influence the adsorption process.²⁸ Proteins may also adsorb to the hydrophilic surfaces due to charge interactions.^{2,29} A number of systematic studies on the protein resistance of different chemical structures of small molecules have been performed and reveal several criteria that have to be fulfilled for a surface to be resistant to proteins.^{30–32} It was proposed that the presence of hydrogen-bond acceptors but not hydrogen-bond donors, an overall neutral charge and hydrophilicity of the material surface are important properties for ensuring resistance to proteins. However, the above-mentioned structural characteristics of nonfouling surfaces are not adequate for the experimental data that has been presented for self-assembled monolayers (SAMs) of OH-terminated PEG^{21,33} or mannitol¹² because they show high resistance to proteins, even though they contain hydrogen-bond donors. Studies of the protein resistance of surfaces modified with mannitol performed by Ostuni et al.³¹

* To whom correspondence should be addressed. Tel.: (+49) 231 755 3860. Fax: (+49) 231 755 3853. E-mail: monika.wyszogrodzka@tu-dortmund.de.

[†] Freie Universität Berlin.

[‡] Technische Universität Dortmund.

on their mixed SAMs show high adsorption of fibrinogen (Fib; ~68%), whereas Luk et al.,¹² who used homogeneous SAMs, found significant reduction of the resistance against Fib to ~2%. These studies suggest that the chain-packing density plays an important role in addition to the above-mentioned requirements.

In spite of many experiments that have attempted to define the physical and chemical requirements for the protein adsorption resistance of PEG, the reasons for these phenomena are still not yet fully understood. Physicists and chemists have proposed several theories, but none of them is adequate to explain its protein-resistant behavior under all the conditions.^{23,34,35} For example, factors like terminal and internal hydrophilicity and the lateral packing density that causes inertness to the proteins.^{30,33} Various studies on short PEG chains performed by Grunze et al.^{22,33,36} have given evidence that the interactions of SAMs based on short PEG chains with water is strongly influenced by their molecular conformation. The authors correlate the molecular conformation of PEG monolayers on gold and silver substrates with their ability to resist protein adsorption. It was found that only the predominantly helical (but not defect-free) conformation of PEG on a gold surface showed high protein resistance, whereas the densely packed "all-trans" monolayer observed on silver adsorbed up to 60% of fibrinogen. Based on these findings, it was concluded that conformational freedom is not a necessary condition for rendering surface resistance to protein adsorption but rather the ability of different conformations to bind water.^{22,36}

Despite the generally accepted theory that water at the protein-PEG interface plays a very important role in protein resistance, the protein repulsion of PEG polymer brushes may arise for different reasons. Andrade and de Gennes^{29,37,38} introduced a "steric repulsion" model that was based on concepts developed for colloid stabilization, which treats proteins as hard spheres and the PEG as random coils. In this model, for the prevention of the protein adsorption, steric repulsion is mainly responsible, resulting from a thermodynamically unfavorable process as the removal of water from the hydrated PEG chains during the compression of PEG layer when the protein comes closer to the surface. Szleifer et al.³⁹⁻⁴² improved a model from Jeon et al.^{37,38} using a single-chain mean field (SCMF) theory. They found that the most important factor for the ability of the polymer layer to prevent protein adsorption is the surface coverage of the grafted polymer, while the chain length had a minor effect.

The molecular mechanisms leading to protein adsorption due to protein-surface interactions are still not fully understood. Nevertheless, Latour³⁵ recently proposed two independently controllable sets of criteria for protein resistance based on the thermodynamic analysis of a system, which include enthalpy, entropy, and free energy changes during the protein adsorption process. Particularly favorable are well-hydrated, long, flexible polymer chains with a packing density that is low enough to allow chain mobility and yet provide complete surface coverage and polymer chains containing hydrogen-bondable groups that are readily accessible to water molecules but not to the hydrogen-bond forming groups of the protein. All these factors may be used to design new materials that resist the adsorption of proteins or to help in understanding the mechanism at the molecular level.

Based on the analysis of the best protein resistant surfaces known in literature^{11,12,20,21,43} it becomes apparent that branched architectures, for example, with highly flexible aliphatic polyether and hydrophilic groups with H-donors are some of the structural features that enable protein resistance and can be found

also in polyglycerol. Our first studies were performed on various hyperbranched polyglycerol (hPG) derivatives, which showed excellent protein resistance against proteins.²⁴ The recently proven high biocompatibility of hPG^{24,44-48} and higher thermal stability²⁴ compared to PEG makes it also attractive for pharmaceutical and biomedical applications. Additionally, the branched architecture with a number of functional groups gives the possibility for further postsynthetic modification and multivalent functionalization.

Unlikely, the mechanism of the anionic polymerization precludes a precise control of the polymer size, architecture, and degree of branching, which complicates a detailed and systematic structure-activity study. Hence, for a better understanding of the underlying mechanisms we decided to synthesize well-defined and monodisperse, dendritic monoamino oligoglycerol derivatives of different generations.^{49,50} It was proven that the amount of the adsorbed proteins strongly depends on the size of the dendrons as well as on its functionality. However, the Whitesides "anhydride" method^{31,51,52} applied there for surface modification did not fulfill our expectations.⁵⁰ Recently, we observed improvements in protein resistance with a higher generation number when grafting monoamino dendrons to a reactive anhydride. This is in contrast to the results obtained for 2,2-bis(hydroxy-methyl)propionic acid (bis-MPA) dendrons, where protein adsorption increases upon dendronization of the PEG surface.⁵³ The highest protein resistance was obtained for a [G2.0] dendron. It was suggested that the observed insufficient coupling (especially for the higher generations, [G3.0] and [G4.0]) was caused by poor accessibility of the amino group and by formation of the hydrogen bonding between hydroxyl groups of the dendrons and carboxylic acid of 11-mercaptoundecanoic acid (MUA) during the coupling step. Therefore, elimination of the hydrogen-donor groups by simple methylation promotes a more efficient coupling and thereby increases the inertness of the surface toward proteins.

Due to the problems of the "anhydride" method arising from the incomplete coupling of sterically demanding amines, we decided to synthesize a library of dendritic polyglycerol alkanethiolates. Because of high reproducibility, self-assembled monolayers based on alkane thiol have been used for an enormous number of applications.⁵⁴⁻⁶² Additionally, alkanethiolates are relatively easy to prepare and they spontaneously form, upon immersion on a gold substrate, a well-defined and ordered SAM and, therefore, are the best model system for this study. This approach allows us, first of all, to exclude the possibility of incomplete coupling and to eliminate unwanted interactions with MUA and, therefore, to obtain more reliable results.

The characterization of the interactions of proteins with surfaces requires a sensitive analytical tool that can measure the rates and amounts of adsorbed proteins. Surface plasmon resonance (SPR) spectroscopy^{63,64} is well suited for this application because of its excellent sensitivity (pg mm^{-2} of adsorbed proteins) and ability to monitor the interaction between molecules and the model proteins (fibrinogen (Fib), pepsin (Pep), albumin (Alb), and lysozyme (Lys))⁶⁵ in real time.

The focus of this study was to investigate the effect of surface functionalization with defined glycerol dendron derivatives on protein adsorption in order to determine: (i) the optimal size (number of generation) necessary to exhibit adsorption of the proteins; (ii) if the elimination of steric hindrance and internal hydrogen bonding improve the coupling and lead to the better monolayers that prevent adsorption of the proteins; and (iii)

whether methylation of all OH-groups has a significant a benefit on protein resistance (like it was shown for sorbitol⁴³).

Experimental Section

General. ¹H NMR and ¹³C NMR spectra were recorded on Bruker AC 250 (250 and 67.5 MHz for ¹H and ¹³C, respectively), ECX 400 (400 and 100 MHz for ¹H and ¹³C, respectively) as well as Delta JEOL Eclipse 500 (500 and 125 MHz for ¹H and ¹³C, respectively) spectrometers at 25 °C. AMX 500 and ECX 400 were used to record high resolution ¹³C NMR. The spectra were calibrated using the solvent peak (CDCl₃, 7.26 ppm for ¹H and 77.0 ppm for ¹³C; CD₃OD, 4.84 ppm for ¹H and 49.05 ppm for ¹³C; acetone-*d*₆, 2.05 ppm for ¹H and 30.83 ppm for ¹³C). Flash chromatography was performed on silica gel 60 (230–400 mesh) using head pressure by means of compressed air. IR spectra were recorded as KBr pellets on a Nicolet 55XC FTIR Interferometer. Elemental analyses were performed on a Perkin-Elmer EA 240. For ESI-TOF measurements an Agilent 6210 ESI-TOF, Agilent Technologies, Santa Clara, U.S.A., and for ESI-FTICR MS (electrospray ionization–Fourier transform ion cyclotron resonance mass spectrometry) measurements, an Ionspec QFT-7, Varian Inc., Lake Forest, U.S.A., were used. HPLC was carried out on a Knauer HPLC (pump K-1800) using a Knauer RI-detector K-2401 and a Nucleosil 50-5 (32 × 240) column.

Reagents. All reagents were purchased from Acros or Aldrich and used as received, unless stated otherwise. Reactions requiring dry conditions were carried out in dried Schlenk glassware under argon. Dry and analytical grade solvents were purchased from Acros or Aldrich and used as received. Triglycerol was obtained as a gift from Solvay Chemicals GmbH and used as received.

SPR Spectroscopy. Fibrinogen (from bovine plasma, F8630), lysozyme (chicken egg white, E.C. 3.2.1.17, L6876), and pepsin (muscle, E.C. 3.4.23.1, P7012) were purchased from Sigma-Aldrich. Bovine serum albumin was obtained from Serva. All proteins were used without further purification. Sodium dodecylsulfate (SDS) was purchased from Acros. Gold substrates were purchased from Biacore (Uppsala, Sweden) and stored at 4–8 °C (SIA Kit). Phosphate buffered saline (10× conc.) was purchased from Cambrex. PBS was freshly prepared by diluting 100 mL of 10× concentrated PBS in 900 mL of Milli-Q water, filtered through 0.22 μm, and degassed at room temp. prior to use (10 mM PO₄³⁻, 138 mM NaCl, 3 mM KCl, pH = 7.4 at 25 °C).

Preparation of Reference SAM. SAMs of hexadecanethiol (HDT) were prepared based on Whitesides' protocol by immersing the gold substrate overnight in a 2 mM ethanolic solution, then rinsed for 30 s with ethanol, and dried under a stream of argon.

Precleaning of the Gold Chips and Preparation of SAMs. The commercial BIAcore (SIA Kit) gold chips were precleaned^{66,67} prior to use by immersion of the chip into the freshly prepared piranha solution for 30 s, then sonicated for 5 min in Milli-Q water, and for an additional 5 min in previously distilled absolute EtOH. The precleaned chip was dried under a stream of argon and immediately immersed into the 1 mM solution of corresponding thiol in ethanol for 0.5–24 h, then rinsed for 30 s with ethanol, and dried in a stream of argon. All chips were immediately used for SPR, CA, and IRRAS experiments.

Protein Adsorption Study by Surface Plasmon Resonance (SPR) Spectroscopy. SPR measurements were performed on a Biacore 3000 instrument (Biacore, Uppsala, Sweden). Protein solution (1 mg/mL in PBS) and SDS solution (1.0% wt in PBS) were freshly prepared and filtered through 0.22 μm filters. The gold chip containing SAMs with our compounds were mounted on a support and inserted into the Biacore 3000. Adsorption of the test proteins to prepared SAMs was measured based on a modified protocol given in ref 50; briefly, (i) flowing a solution of SDS (1.0 wt % in PBS) over the SAM surface for 3 min and then rinsing the surface with PBS buffer for 10 min; (ii) flowing solution of the adequate protein (1 mg/mL in PBS) for 30 min; and finally, (iii) allowing PBS buffer to flow over the surface for additional 10 min. The flow rate used for all experiments was 10 μL/min.

Proteins. We examined the adsorption of the four model proteins due to their properties (molecular weight and pI) and behavior under the conditions of our experiment (phosphate buffered saline, PBS, pH = 7.4). (i) Fibrinogen (Fib, 340 kDa, pI 5.5) is a large, blood plasma protein that strongly adsorbs to hydrophobic surfaces, commonly used as a model for sticky serum proteins; (ii) albumin (Alb, 65 kDa, pI 4.8) is the most abundant protein in the human blood circulatory system (~65%), contributes 80% to colloid osmotic blood pressure and is negatively charged under physiological conditions; (iii) lysozyme (Lys, 14 kDa, pI 11.0) is a small, positively charged protein, used as a model for electrostatic interactions of proteins with surfaces; and (iv) pepsin (Pep, 34 kDa, pI < 2.0), is a relatively small and negatively charged protein (enzyme from the stomach) used as a model protein as opposed to positively charged Lys.

Contact Angle Measurements. The water contact angles on the SAMs were measured with a Contact Angle System OCA20 from DataPhysics Instruments GmbH. Liquid drops (Milli-Q water) were delivered to the surface using micrometer syringe. The reported values of the contact angles are calculated with Young–Laplace method from an average of 3–5 different measurements taken at different locations on the surface.

XPS Measurements. X-ray photoelectron spectroscopy measurements were realized by means of a SPECS Phoibos 100 electron analyzer at a typical energy resolution of 600 meV at 20 eV pass energy. An Mg K_α X-ray tube has been used as light source, with an excitation photon energy of 1253.6 eV and a photon resolution of 800 meV. The binding energies have been calibrated to the Au 4f_{7/2} binding energy at 84.0 eV. The electron takeoff angle was set to 0°, corresponding with normal emission. The peak line profile was chosen as the product of a Gaussian function and a Lorentzian one. Quantitative analysis was performed using Shirley background subtraction and subsequent numerical integration.

Synthesis. General Procedure for Ether Formation. Procedure A. A total of 4.0 equiv per -OH group of freshly powdered KOH was added to the anhydrous DMSO. After stirring for 5 min, an alcohol was added to the solution and allowed to stir for an additional 5 min. Finally, 2.0 equiv per -OH of 11-bromoundecene (or CH₃I, when methylation of the dendrons were performed) was added and stir for 30–45 min. Reaction was quenched by addition of water, followed by extraction with CH₂Cl₂. The combined organic layers were dried over Na₂SO₄, filtered, and concentrated under vacuum. Purification of the residue by column chromatography gives the desired compounds in high yield.

Procedure B. [Gn]-OH (1.0 equiv), 60% NaH (2.5–5.0 equiv) in mineral oil, cat. amount of 15-C-5, and freshly distilled dry THF were placed in a dry two-necked round bottomed flask under an Ar atmosphere. After 2–3 h stirring at 40 °C, 11-bromoundecene (2.0 equiv), cat. amount of KI, and 18-C-6 were added to the solution. The mixture was stirred under reflux for 12–24 h. After cooling to room temp., the reaction was quenched with distilled water and extracted with CH₂Cl₂. The organic layer then was dried over Na₂SO₄ and solvent was removed under vacuum. Purification of the residue was done by silica gel column chromatography giving the desired product in high yield.

*C*₁₁-[G1.0] (5a). Compound **5a** was synthesized according to the Procedure A, followed by silica gel column chromatography with *n*-hexane/EtOAc (4:1, v/v), yielding **5a** (63%). ¹H NMR (500 MHz, CDCl₃, 25 °C): δ = 5.78 (tdd, 1 H, *J* = 6.7, 10.2, 16.9 Hz, CH₂CHCH₂), 4.96 (ddd, 1 H, *J* = 1.6, 3.6, 17.1 Hz, CH₂CHCH₂), 4.90 (tdd, 1 H, *J* = 1.2, 2.2, 10.2 Hz, CH₂CHCH₂), 4.23 (d p, 2 H, *J* = 2.3, 6.0 Hz, OCH₂CHCH₂O), 4.02 (dd, 2 H, *J* = 6.4, 8.2 Hz), 3.71 (dd, 1 H, *J* = 6.4, 8.3 Hz), 3.46 (ddd, 3 H, *J* = 5.7, 8.2, 10.0 Hz), 3.39 (t, 1 H, *J* = 6.7 Hz, CH₂CH₂O), 2.01 (dd, 2 H, *J* = 6.9, 14.5 Hz, CH₂CHCH₂), 1.52 (m, 2 H), 1.38 (s, 6 H, CH₃), 1.32 (br, 2 H, CH₂CH₂), 1.28 (s, 6 H, CH₃), 1.25 (br, 10 H, CH₂CH₂) ppm. ¹³C NMR (125 MHz, CDCl₃, 25 °C): δ = 139.1, 114.0, 109.3, 78.6, 77.7, 74.6, 72.4, 71.6, 71.3, 70.6, 66.9, 66.8, 66.7, 71.8, 70.8, 68.6, 68.4, 33.7, 30.0, 29.5, 28.9,

26.7, 26.0, 25.4 ppm. ESI-TOF MS Calcd. for $C_{26}H_{48}O_7$; 472.3400; found, 473.3468 [M + H]⁺, 490.3734 [M + NH₄]⁺, 495.3290 [M + Na]⁺, 511.3028 [M + K]⁺. Anal. Calcd for $C_{26}H_{48}O_7$: C, 66.07; H, 10.24. Found: C, 66.16; H, 10.32.

C₁₁-[G2.0] (5b). Compound **5b** was synthesized according to the Procedure A, followed by silica gel column chromatography with *n*-hexane/EtOAc (1:1, v/v), yielding **5b** (50%). ¹H NMR (250 MHz, CDCl₃, 25 °C): δ = 5.76 (tdd, 1 H, *J* = 6.6, 10.1, 16.9 Hz, CH₂CHCH₂), 4.97–4.85 (m, 2 H, CH₂CHCH₂), 4.19 (p, 4 H, *J* = 5.9 Hz), 4.01 (m, 4 H), 3.69 (m, 4 H), 3.53 (br m, 25 H, CH₂CHO backbone), 2.00 (q, 2 H, *J* = 6.6 Hz, CH₂CHCH₂), 1.50 (m, 4 H), 1.38 (s, 12 H, CH₃), 1.32 (s, 12 H, CH₃), 1.24 (br s, 10 H, CH₂CH₂) ppm. ¹³C NMR (67.5 MHz, CDCl₃, 25 °C): δ = 139.09, 114.05, 109.25, 78.61, 78.38, 78.20, 77.9, 74.71, 74.56, 72.42, 71.46, 71.29, 70.46, 70.30, 66.89, 66.74, 33.72, 30.08, 29.51, 29.45, 29.40, 29.05, 28.85, 26.71, 26.06, 25.36 ppm. ESI-TOF MS Calcd. for $C_{44}H_{80}O_{15}$; 848.5497; found, 849.5573 [M + H]⁺, 871.5395 [M + Na]⁺, 887.5133 [M + K]⁺. Anal. Calcd for $C_{44}H_{80}O_{15}$: C, 62.24; H, 9.50. Found: C, 62.54; H, 9.11.

C₁₁-[G3.0] (5c). Compound **5c** was synthesized according to the Procedure B, followed by silica gel column chromatography with 25% propanol in *n*-hexane, yielding **5c** (66%). ¹H NMR (400 MHz, CDCl₃, 25 °C): δ = 5.77 (m, 1 H, CH₂CHCH₂), 4.95–4.91 (m, 1 H, CH₂CHCH₂), 4.88–4.86 (m, 1 H, CH₂CHCH₂), 4.18 (m, 8 H), 3.98 (m, 8 H), 3.67 (m, 8 H), 3.62–3.38 (br m, 54 H, CH₂CHO backbone), 2.00 (m, 2 H, CH₂CHCH₂), 1.47 (m, 2 H, CH₂CH₂), 1.36 (s, 24 H, CH₃), 1.30 (s, 24 H, CH₃), 1.22 (br s, 12 H, CH₂CH₂) ppm. ¹³C NMR (100 MHz, CDCl₃, 25 °C): δ = 139.22, 114.23, 109.42, 78.75, 78.44, 74.84, 74.68, 72.57, 71.69, 71.50, 71.32, 70.69, 70.21, 67.02, 66.90, 66.89, 33.89, 30.33, 29.72, 29.61, 29.24, 29.14, 29.02, 26.92, 26.27, 25.52 ppm. ESI-TOF MS Calcd. for $C_{80}H_{144}O_{31}$; 1600.9692; found, 1619.0037 [M + NH₄]⁺, 1623.9595 [M + Na]⁺, 1639.9339 [M + K]⁺. Anal. Calcd for $C_{80}H_{144}O_{31}$: C, 59.98; H, 9.06. Found: C, 59.61; H, 8.81.

C₁₁-[G1.0]-OMe (7a). Compound **7a** was synthesized according to the Procedure A, filtration through thin layer of silica gel with *n*-hexane/EtOAc (1:1, v/v), yielding **7a** (83%). ¹H NMR (500 MHz, CDCl₃, 25 °C): δ = 5.75 (tdd, 1 H, *J* = 6.7, 10.2, 16.9 Hz, CH₂CHCH₂), 4.96 (ddd, 1 H, *J* = 1.8, 3.5, 17.1 Hz, CH₂CHCH₂), 4.87 (m, 1 H, CH₂CHCH₂), 3.32 (m, 1 H), 3.55–3.36 (m, 17 H, CH₂CHO backbone), 3.41 (s, 6 H, OCH₃), 3.32 (s, 6 H, OCH₃), 1.98 (q, 2 H, *J* = 7.2 Hz, CH₂CHCH₂), 1.54 (m, 2 H, CH₂CH₂O), 1.32 (m, 2 H, CH₂CH₂), 1.23 (br s, 10 H, CH₂CH₂) ppm. ¹³C NMR (125 MHz, CDCl₃, 25 °C): δ = 139.02, 114.0, 79.28, 79.09, 78.55, 77.60, 72.30, 71.48, 71.40, 70.89, 70.83, 70.52, 69.56, 59.12, 57.85, 57.75, 33.67, 29.99, 29.56, 29.43, 29.33, 28.99, 28.80, 25.98 ppm. ESI-TOF MS Calcd. for $C_{24}H_{48}O_7$; 448.3400; found, 449.3472 [M + H]⁺, 471.3294 [M + Na]⁺.

C₁₁-[G2.0]-OMe (7b). Compound **7b** was synthesized according to the Procedure A, followed by filtration through a thin layer of silica gel with *n*-hexane/EtOAc (1:1, v/v), yielding **7b** (>99%). ¹H NMR (500 MHz, CDCl₃, 25 °C): δ = 5.78 (tdd, 1 H, *J* = 6.7, 10.2, 16.9 Hz, CH₂CHCH₂), 4.96 (ddd, 1 H, *J* = 1.6, 3.6, 17.1 Hz, CH₂CHCH₂), 4.90 (tdd, 1 H, *J* = 1.2, 2.3, 10.2 Hz, CH₂CHCH₂), 3.64 (m, 2 H), 3.60 (m, 4 H), 3.54–3.39 (br m, 31 H, CH₂CHO backbone), 3.45 (s, 12 H, OCH₃), 3.34 (s, 12 H, OCH₃), 2.01 (dd, 2 H, *J* = 6.8, 14.6 Hz, CH₂CHCH₂), 1.51 (m, 2 H, CH₂CH₂O), 1.34 (m, 2 H), 1.24 (br s, 10 H, CH₂CH₂) ppm. ¹³C NMR (125 MHz, CDCl₃, 25 °C): δ = 139.11, 114.05, 79.34, 79.14, 78.57, 78.36, 72.32, 71.73, 71.65, 71.38, 70.58, 70.49, 70.37, 69.72, 59.20, 57.92, 33.74, 30.11, 29.53, 29.48, 29.42, 29.07, 28.87, 26.08 ppm. ESI-TOF MS Calcd. for $C_{40}H_{80}O_{15}$; 800.5497; found, 801.5587 [M + H]⁺, 818.5846 [M + NH₄]⁺, 823.5402 [M + Na]⁺, 839.5141 [M + K]⁺. Anal. Calcd for $C_{40}H_{80}O_{15}$: C, 59.97; H, 10.07. Found: C, 60.22; H, 10.06.

C₁₁-[G3.0]-OMe (7c). Compound **7c** was synthesized according to the Procedure A, followed by filtration through a thin layer of silica gel with 5% MeOH in CH₂Cl₂, yielding **7c** (83%). ¹H NMR (500 MHz, CDCl₃, 25 °C): δ = 5.77 (tdd, 1 H, *J* = 6.7, 9.9, 16.9 Hz, CH₂CHCH₂), 4.96 (d, 1 H, *J* = 17.1 Hz, CH₂CHCH₂), 4.89 (d, 1 H, *J* = 10.2 Hz,

CH₂CHCH₂), 3.64–3.39 (br m, 101 H, CH₂CHO backbone), 3.42 (s, 24 H, OCH₃), 3.33 (s, 24 H, OCH₃), 2.00 (dd, 2 H, *J* = 6.8, 13.7 Hz, CH₂), 1.49 (m, 2 H, CH₂CH₂O), 1.33 (m, 2 H, CH₂), 1.24 (br s, 10 H, CH₂CH₂) ppm. ¹³C NMR (100 MHz, CDCl₃, 25 °C): δ = 139.08, 114.08, 79.29, 79.09, 78.55, 78.25, 72.27, 71.42, 71.19, 70.95, 70.91, 70.55, 70.08, 69.72, 59.20, 57.92, 57.82, 33.74, 30.19, 29.59, 29.47, 29.10, 28.87, 26.13 ppm. ESI-TOF MS Calcd. for $C_{72}H_{144}O_{31}$; 1504.9692; found, 1527.9582 [M + Na]⁺.

General Procedure for the Deprotection of the Alcohol/Acetate Functionality. To 1.0 equiv of acetal/thioacetate protected compounds dissolved in MeOH was added ionic exchange resin Dowex 50W and the mixture refluxed for 12–24 h. After cooling down, Dowex 50W was filtered off and washed with MeOH, and the residue was concentrated under vacuum, yielding the desired compound in 88–99%.

C₁₁-[G1.0]-OH (6a). Reaction conditions and workup were as described above. Evaporation of the solvent gives the desired product **6a** (>99%). ¹H NMR (500 MHz, MeOD, 25 °C): δ = 5.78 (tdd, 1 H, *J* = 6.7, 10.2, 17.0 Hz, CH₂CHCH₂), 4.96 (m, 1 H, CH₂CHCH₂), 4.90 (m, 1 H, CH₂CHCH₂), 3.72 (m, 2 H), 3.60–3.49 (m, 13 H, CH₂CHO backbone), 3.44 (m, 2 H), 2.02 (q, 2 H, *J* = 6.7 Hz, CH₂CHCH₂), 1.54 (m, 2 H, CH₂CH₂O), 1.35 (m, 4 H, CH₂), 1.29 (br s, 8 H, CH₂CH₂) ppm. ¹³C NMR (125 MHz, MeOD, 25 °C): δ = 140.17, 114.75, 79.22, 74.02, 73.95, 72.21, 71.57, 64.50, 34.94, 31.15, 30.74, 30.61, 30.26, 30.16, 27.22 ppm. ESI-TOF MS Calcd. for $C_{20}H_{40}O_7$; 392.2774; found, 393.2837 [M + H]⁺, 415.2657 [M + Na]⁺.

C₁₁-[G2.0]-OH (6b). Reaction conditions and workup were as described above. Evaporation of the solvent gives the desired product **6b** (>99%). ¹H NMR (500 MHz, MeOD, 25 °C): δ = 5.79 (tdd, 1 H, *J* = 6.7, 10.2, 17.0 Hz, CH₂CHCH₂), 4.96 (qd, 1 H, *J* = 1.6, 17.1 Hz, CH₂CHCH₂), 4.89 (m, 1 H, CH₂CHCH₂), 3.37 (m, 6 H), 3.66 (m, 4 H), 3.61–3.44 (br m, 27 H, CH₂CHO backbone), 2.03 (q, 2 H, *J* = 7.0 Hz, CH₂CHCH₂), 1.54 (m, 2 H, CH₂CH₂O), 1.36 (m, 4 H, CH₂), 1.24 (br, 8 H, CH₂CH₂) ppm. ¹³C NMR (100 MHz, MeOD, 25 °C): δ = 140.17, 114.75, 79.88, 73.98, 72.97, 72.47, 72.33, 72.24, 71.50, 71.44, 71.07, 64.52, 33.7, 31.19, 30.76, 30.65, 30.62, 30.26, 30.16, 27.28 ppm. ESI-TOF MS Calcd. for $C_{32}H_{64}O_{15}$; 688.4245; found, 689.4315 [M + H]⁺, 711.4138 [M + Na]⁺, 727.3828 [M + K]⁺. Anal. Calcd for $C_{32}H_{64}O_{15}$: C, 55.80; H, 9.36. Found: C, 56.04; H, 9.05.

C₁₁-[G3.0]-OH (6c). Reaction conditions and workup were as described above. Evaporation of the solvent gives the desired product **6c** (98%). ¹H NMR (500 MHz, MeOD, 25 °C): δ = 5.79 (tdd, 1 H, *J* = 6.7, 10.2, 17.0 Hz, CH₂CHCH₂), 4.97 (qd, 1 H, *J* = 1.6, 17.1 Hz, CH₂CHCH₂), 4.89 (m, 1 H, CH₂CHCH₂), 3.75 (m, 8 H), 3.67 (m, 12 H), 3.62–3.44 (br m, 55 H, CH₂CHO backbone), 2.03 (q, 2 H, *J* = 6.8 Hz, CH₂CHCH₂), 1.55 (m, 2 H, CH₂CH₂O), 1.36 (m, 4 H, CH₂), 1.30 (br, 8 H, CH₂CH₂) ppm. ¹³C NMR (100 MHz, MeOD, 25 °C): δ = 140.10, 114.80, 79.79, 79.74, 79.68, 73.94, 73.90, 72.91, 72.41, 72.36, 72.24, 72.14, 71.42, 70.98, 64.48, 64.47, 34.86, 31.19, 30.74, 30.64, 30.58, 30.21, 30.09, 27.26 ppm. ESI-TOF MS Calcd. for $C_{56}H_{112}O_{31}$; 1280.7188; found, 1304.7074 [M + Na]⁺, 1319.6778 [M + K]⁺.

HS-C₁₁-[G1.0]-OH (1a). Reaction conditions and workup were as described above. Evaporation of the solvent gives the desired product **1a** (>99%). ¹H NMR (500 MHz, CD₃OD, 25 °C): δ = 3.74 (m, 2 H), 3.65 (m, 1 H), 3.61–3–43 (br m, 15 H, CH₂CHO backbone), 2.47 (t, 2 H, *J* = 7.2 Hz, HSCH₂), 1.55 (m, 4 H, HSCH₂CH₂, CH₂CH₂O), 1.29 (br m, 14 H, CH₂CH₂) ppm. ¹³C NMR (100 MHz, CD₃OD, 25 °C): δ = 79.89, 79.85, 79.16, 73.98, 73.91, 72.96, 72.89, 72.66, 72.47, 72.42, 72.17, 71.72, 71.52, 64.47, 64.46, 35.24, 35.24, 31.12, 30.74, 30.68, 30.61, 30.24, 29.45, 27.20, 25.03 ppm. ESI-TOF MS Calcd. for $C_{20}H_{42}O_7S$; 426.2651; found, 449.2560 [M + Na]⁺.

HS-C₁₁-[G1.0]-OMe (2a). Reaction conditions and workup were as described above. Evaporation of the solvent gives the desired product **2a** (93%). ¹H NMR (400 MHz, CDCl₃, 25 °C): δ = 3.65 (m, 1 H, OCH(CH₂O)₂), 4.55–3.38 (br m, 16 H, CH₂CHO backbone), 3.43 (s, 6 H, OCH₃), 3.34 (s, 6 H, OCH₃), 2.49 (q, 2 H, *J* = 7.4 Hz, HSCH₂), 1.57 (m, 4 H, HSCH₂CH₂, CH₂CH₂O), 1.22 (br m, 15 H, CH₂CH₂, HS) ppm. ¹³C NMR (100 MHz, CDCl₃, 25 °C): δ = 79.31, 79.13,

78.58, 77.63, 72.34, 71.57, 71.52, 71.44, 70.94, 70.87, 70.57, 69.60, 59.18, 57.90, 57.80, 33.96 (HSCH₂), 30.03, 29.60, 29.49, 29.41, 28.98, 26.02, 24.55 ppm. ESI-TOF MS Calcd. for C₂₄H₅₀O₇S, 482.3277; found, 505.3196 [M + Na]⁺, 521.2960 [M + K]⁺.

HS-C₁₁-[G2.0]-OH (1b). Reaction conditions and workup were as described above. Evaporation of the solvent gives the desired product **1b** (90%). ¹H NMR (500 MHz, CD₃OD, 25 °C): δ = 3.73 (m, 5 H), 3.65 (m, 4 H), 3.60–3.43 (br m, 28 H, CH₂CHO backbone), 2.47 (t, 2 H, J = 7.1 Hz, HSCH₂), 1.55 (m, 4 H, HSCH₂CH₂, CH₂CH₂O), 1.29 (br m, 14 H, CH₂CH₂) ppm. ¹³C NMR (100 MHz, CD₃OD, 25 °C): δ = 79.83, 79.36, 73.97, 73.93, 72.92, 72.41, 72.28, 72.19, 71.01, 64.48, 64.43, 35.24 (HSCH₂), 31.16, 30.69, 30.24, 29.44, 27.25, 25.02 ppm. ESI-TOF MS Calcd. for C₃₂H₆₆O₁₅S, 722.4122; found, 745.4012 [M + Na]⁺.

HS-C₁₁-[G2.0]-OMe (2b). Reaction conditions and workup were as described above. Evaporation of the solvent gives the desired product **2b** (>99%). ¹H NMR (500 MHz, CDCl₃, 25 °C): δ = 3.63–3.38 (br m, 37 H, CH₂CHO backbone), 3.41 (s, 12 H, OCH₃), 3.32 (s, 12 H, OCH₃), 2.49 (dd, 2 H, J = 7.5, 14.7 Hz, HSCH₂), 1.57 (m, 4 H, HSCH₂CH₂, CH₂CH₂O), 1.22 (br m, 15 H, CH₂CH₂, HS) ppm. ¹³C NMR (125 MHz, CDCl₃, 25 °C): δ = 79.30, 79.11, 78.54, 78.39, 78.33, 72.29, 71.68, 71.31, 70.90, 70.45, 70.33, 69.69, 59.17, 57.89, 57.79, 33.95 (HSCH₂), 30.08, 29.51, 29.47, 29.094, 28.98, 28.74, 28.28, 26.06, 24.54 ppm. ESI-TOF MS Calcd. for C₄₀H₈₂O₁₅S, 834.5374; found, 857.5273 [M + Na]⁺.

HS-C₁₁-[G3.0]-OH (1c). Reaction conditions and workup were as described above. Evaporation of the solvent gives the desired product **1c** (96%). ¹H NMR (500 MHz, CD₃OD, 25 °C): δ = 3.72 (m, 10 H), 3.65 (m, 12 H), 3.60–3.43 (br m, 55 H, CH₂CHO backbone), 2.44 (t, 2 H, J = 7.1 Hz, HSCH₂), 1.53 (m, 4 H, HSCH₂CH₂, CH₂CH₂O), 1.27 (br m, 14 H, CH₂CH₂) ppm. ¹³C NMR (100 MHz, CD₃OD, 25 °C): δ = 80.27, 80.01, 79.86, 79.75, 74.00, 73.96, 72.97, 72.46, 72.30, 72.20, 71.49, 71.05, 64.51, 35.25 (HSCH₂), 31.26, 30.82, 30.72, 30.27, 29.45, 27.33, 25.02 ppm. ESI-TOF MS Calcd. for C₅₆H₁₁₄O₃₁S, 1314.7065; found, 1337.6930 [M + Na]⁺.

(S-C₁₁-[G3.0]-OMe)₂ (2c). A solution of the thioacetate in methanol was purged with Ar, after which 5 equiv of 30% NaOMe in MeOH were added. After 30 min, the reaction mixture was neutralized with Dowex 50W and filtered. Evaporation and purification with flash chromatography (10% MeOH in EtOAc) yielded the final product **2c** (20%). ¹H NMR (500 MHz, CD₃OD, 25 °C): δ = 3.73–3.42 (br m, 154 H, CH₂CHO backbone), 3.44 (s, 48 H, OCH₃), 3.35 (s, 48 H, OCH₃), 2.69 (t, 4 H, J = 7.2 Hz, SCH₂CH₂), 1.68 (m, 4 H, SCH₂CH₂), 1.56 (p, 4 H, J = 6.5 Hz, CH₂CH₂O), 1.22 (br m, 28 H, CH₂CH₂) ppm. ¹³C NMR (100 MHz, CD₃OD, 25 °C): δ = 80.7, 80.64, 80.03, 79.92, 79.87, 73.39, 72.47, 72.14, 71.48, 71.27, 70.91, 59.57, 58.34, 39.79 (SCH₂CH₂), 31.39, 30.89, 30.77, 30.44, 30.29, 29.56, 27.43 ppm. ESI-TOF MS Calcd. for C₁₄₄H₂₉₀O₆₂S₂, 3075.8981; found, 1048.2929 [M + 3Na]⁺, 1560.9436 [M + 2Na]⁺.

General Procedure for the Thioacetylation. To 1.0 equiv of alkene compound dissolved in dry THF was added 10.0 equiv of AcSH and irradiated for 1 h. Reaction mixture was concentrated under vacuum and the residue purified by column chromatography gives compounds **8** and **9** in high yield.

AcS-C₁₁-[G1.0] (8a). Reaction conditions and workup were as described above. Silica gel column chromatography with EtOAc/*n*-hexane (1:1, v/v) gives the desired product **8a** in 70%. ¹H NMR (500 MHz, CDCl₃, 25 °C): δ = 4.24 (d p, 2 H, J = 2.3, 6.0 Hz), 4.02 (dd, 2 H, J = 6.4, 8.2 Hz), 3.71 (dd, 2 H, J = 6.4, 8.3 Hz), 3.72 (m, 1 H), 3.64–3.40 (br m, 10 H), 3.39 (t, 1 H, J = 6.7 Hz, CH₂O), 2.84 (m, 2 H, SCH₂), 2.31 (s, 3 H, CH₃COS), 1.54 (qd, 4 H, J = 6.8, 13.2 Hz, SCH₂CH₂, CH₂CH₂O), 1.40 (s, 6 H, CH₃), 1.34 (s, 6 H, CH₃), 1.24 (br, 14 H, CH₂CH₂) ppm. ¹³C NMR (125 MHz, CDCl₃, 25 °C): δ = 196.11, 109.41, 78.78, 77.80, 74.73, 72.54, 71.70, 71.47, 70.75, 70.71, 67.06, 66.88, 30.72, 30.15, 29.65, 29.58, 29.54, 29.22, 29.19, 28.89, 26.85, 26.16, 25.51 ppm. QFT-ESI MS Calcd. for C₂₈H₅₂O₈S, 548.3383; found, 571.3273 [M + Na]⁺.

AcS-C₁₁-[G1.0]-OMe (9a). Reaction conditions and workup were as described above. Silica gel column chromatography with EtOAc/*n*-hexane (1:2, v/v) gives the desired product **9a** in 81% yield. ¹H NMR (500 MHz, CDCl₃, 25 °C): δ = 3.64 (m, 1 H), 4.55–3.37 (br m, 16 H, CH₂CHO backbone), 3.42 (s, 6 H, OCH₃), 3.33 (s, 6 H, OCH₃), 2.81 (t, 2 H, J = 7.3 Hz, SCH₂), 2.28 (s, 3 H, CH₃COS), 1.51 (m, 4 H, SCH₂CH₂, CH₂CH₂O), 1.22 (br m, 14 H, CH₂CH₂) ppm. ¹³C NMR (125 MHz, CDCl₃, 25 °C): δ = 196.08, 79.44, 79.26, 78.72, 77.77, 72.48, 71.65, 71.06, 70.99, 70.74, 69.73, 59.34, 58.06, 30.71, 30.18, 29.65, 29.57, 29.20, 29.18, 28.88, 26.18 ppm. ESI-TOF MS Calcd. for C₂₆H₅₂O₈S, 524.3383; found, 525.3479 [M + H]⁺, 547.3298 [M + Na]⁺, 563.3035 [M + K]⁺.

AcS-C₁₁-[G2.0] (8b). Reaction conditions and workup were as described above. Silica gel column chromatography with 25% 2-propanol in *n*-hexane gives the desired product **8b** in >99%. ¹H NMR (500 MHz, CDCl₃, 25 °C): δ = 4.21 (m, 4 H), 4.02 (dd, 4 H, J = 6.4, 8.2 Hz), 3.70 (dd, 4 H, J = 6.5, 8.1 Hz), 3.65–3.43 (br m, 27 H, CH₂CHO backbone), 2.83 (t, 2 H, J = 7.4 Hz, SCH₂), 2.30 (s, 3 H, CH₃COS), 1.51 (m, 4 H, SCH₂CH₂, CH₂CH₂O), 1.39 (s, 12 H, CH₃), 1.33 (s, 12 H, CH₃), 1.24 (br, 12 H, CH₂CH₂) ppm. ¹³C NMR (100 MHz, CDCl₃, 25 °C): δ = 195.92, 109.27, 78.61, 78.38, 78.20, 77.97, 74.72, 74.57, 72.43, 71.55, 71.47, 71.29, 70.49, 70.30, 66.89, 66.76, 30.58, 30.10, 29.56, 29.49, 29.44, 29.073, 28.76, 26.73, 26.08, 25.37 ppm. ESI-TOF MS Calcd. for C₄₆H₈₄O₁₆S, 924.5480; found, 947.5362 [M + Na]⁺, 963.5106 [M + K]⁺.

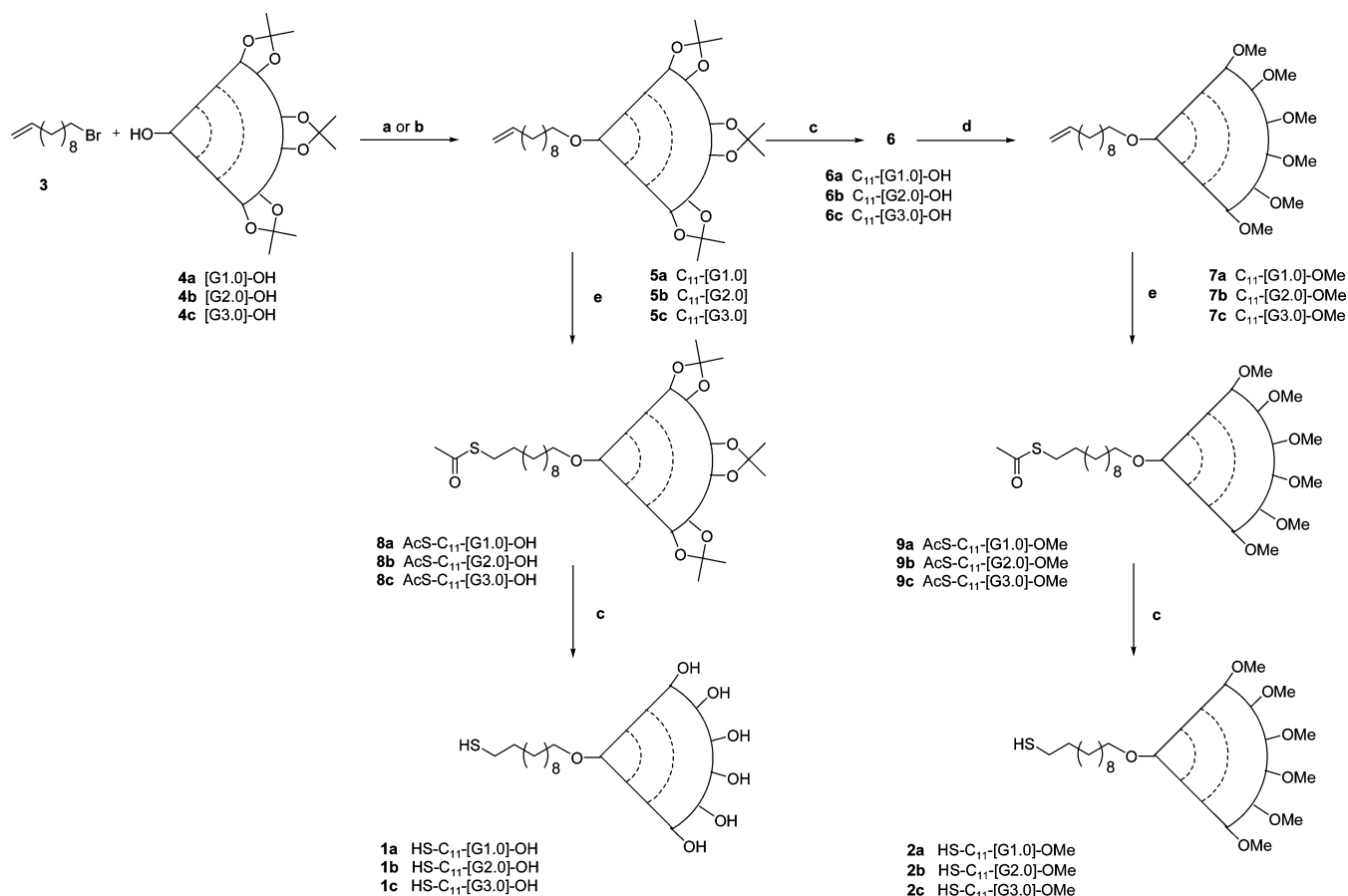
AcS-C₁₁-[G2.0]-OMe (9b). Reaction conditions and workup were as described above. Silica gel column chromatography with 5% MeOH in CH₂Cl₂ gives the desired product **9b** in 95% yield. ¹H NMR (500 MHz, CDCl₃, 25 °C): δ = 3.64–3.38 (br m, 37 H, CH₂CHO backbone), 3.42 (s, 12 H, OCH₃), 3.33 (s, 12 H, OCH₃), 2.81 (t, 2 H, J = 7.3 Hz, SCH₂), 2.28 (s, 3 H, CH₃COS), 1.49 (m, 4 H, SCH₂CH₂, CH₂CH₂O), 1.22 (br m, 14 H, CH₂CH₂) ppm. ¹³C NMR (125 MHz, CDCl₃, 25 °C): δ = 196.08, 79.32, 79.13, 78.56, 78.35, 78.02, 72.32, 71.72, 71.34, 70.96, 70.91, 69.71, 59.22, 57.93, 57.83, 30.58, 30.12, 29.51, 29.43, 29.07, 28.77, 26.09 ppm. ESI-TOF MS Calcd. for C₄₀H₈₀O₁₅, 876.5480; found, 894.5796 [M + NH₄]⁺, 899.5353 [M + Na]⁺.

AcS-C₁₁-[G3.0] (8c). Reaction conditions and workup were as described above. Silica gel column chromatography with 25% 2-propanol in *n*-hexane gives the desired product **8c** in 82% yield. ¹H NMR (500 MHz, CDCl₃, 25 °C): δ = 4.19 (m, 8 H, CH(O)CH₂O), 4.02 (dd, 8 H, J = 6.4, 8.2 Hz, CH(O)CH₂O), 3.68 (m, 10 H, J = 6.5, 8.1 Hz, CH(O)CH₂O), 3.65–3.43 (br m, 51 H, CH₂CHO backbone), 2.82 (t, 2 H, J = 7.4 Hz, SCH₂), 2.28 (s, 3 H, CH₃COS), 1.52 (m, 4 H, SCH₂CH₂, CH₂CH₂O), 1.36 (s, 26 H, CH₃), 1.31 (s, 24 H, CH₃), 1.22 (br s, 12 H, CH₂CH₂) ppm. ¹³C NMR (100 MHz, CDCl₃, 25 °C): δ = 195.81, 109.21, 78.75, 78.56, 78.33, 74.66, 74.50, 72.40, 71.61, 71.50, 71.33, 71.15, 70.50, 70.03, 66.84, 66.71, 30.52, 30.16, 29.53, 29.41, 29.03, 28.73, 26.71, 26.11, 25.34 ppm. ESI-TOF MS Calcd. for C₈₂H₁₄₈O₃₂S, 1676.9675; found, 1699.9576 [M + Na]⁺.

AcS-C₁₁-[G3.0]-OMe (9c). Reaction conditions and workup were as described above. Silica gel column chromatography with 10% ethyl acetate in *n*-hexane gives the desired product **9c** in 50% yield. ¹H NMR (400 MHz, CDCl₃, 25 °C): δ = 3.66–3.38 (br m, 77 H, CH₂CHO backbone), 3.40 (s, 24 H, OCH₃), 3.32 (s, 24 H, OCH₃), 2.81 (t, 2 H, J = 7.3 Hz, SCH₂), 2.27 (s, 3 H, CH₃COS), 1.47 (m, 4 H, SCH₂CH₂, CH₂CH₂O), 1.22 (br m, 14 H, CH₂CH₂) ppm. ¹³C NMR (125 MHz, CDCl₃, 25 °C): δ = 195.89, 79.25, 79.05, 78.75, 78.51, 78.22, 72.23, 71.35, 71.15, 70.88, 70.51, 70.04, 69.67, 59.15, 57.87, 30.53, 30.16, 29.55, 29.41, 29.03, 28.72, 28.42, 26.10 ppm. ESI-TOF MS Calcd. for C₇₄H₁₄₈O₃₂S, 1580.9675; found, 1603.9574 [M + Na]⁺.

Results and Discussion

Synthesis of Thiolated Dendritic Polyglycerol Derivatives. Recently, we reported on the synthesis of polyglycerol dendrons, which can be achieved by either the divergent or the convergent growth approach.^{49,68,69} The later, well-optimized

Scheme 1. Synthesis of Alkanethiol Polyglycerol Dendrons:^a

^a Reagents and conditions: (a) KOH, DMSO; (b) NaH, THF; (c) H⁺, MeOH; (d) KOH, CH₃I, DMSO; (e) AcSH, AIBN, hν, THF.

convergent pathway provides an efficient access to bifunctional glycerol dendrons [G1.0]–[G3.0] on a multigram scale.⁶⁸

By applying Williamson's ether synthesis, the alkene-terminated polyglycerol dendrons **5a–c** were prepared and served as starting materials for the synthesis of thiol-function-alized glycerol dendrons **1** and **2a–c**. Compounds **5a** and **5b** were easily obtained by reaction of [Gn]-OH⁶⁸ (**4a** or **4b**) with 4.0 equiv of powdered KOH and 2.0 equiv of 11-bromoundecene in anhydrous DMSO at room temp. for a max. of 0.5 h (Scheme 1). Unfortunately, the conversion of **4c** to the coupling product with this method was not quantitative, which is required to avoid tedious purification. Therefore, compound **5c** was synthesized by reaction of 1.0 equiv of **4c** with a suspension of NaH and 2.0 equiv of 11-bromoundecene in dry THF under reflux in the presence of catalytic amounts of KI, 15-crown-5, and 18-crown-6.

Stirring **5a–c** with acidic ion-exchange resin in methanol lead to the quantitative removal of the acetal protecting groups and gives the desired compounds **6a–c**. According to the procedure described previously,⁵⁰ methylation of the free hydroxyl groups lead to the methylated PG-alkenes **7a–c**. Then, thioacetylation was achieved in a photoreaction with thioacetic acid in THF using AIBN as radical initiator.²⁰ The reaction mixture was irradiated for 1 h with a 150 W high pressure mercury lamp, giving the compounds **8a–c** and **9a–c** in nearly quantitative yields. To avoid oxidation of the thiol to the corresponding disulfide (elucidated by ¹H NMR spectroscopy and MS), methanolysis of the thioacetate was carried out using an acidic ion-exchange resin in methanol overnight under reflux. In addition, within one reaction step the acetal deprotection of the

terminal alcohol groups was achieved for compounds **1a–c**. The same thioacetate coupling procedure was applied for the methylated compounds **9a–c**. Unfortunately, in the case of compound **9c**, only traces of the product **2c** (as detected by ESI-MS) were obtained after 48 h reflux. Therefore, we decided to use a well-known procedure for the removal of acetate with NaOMe.⁷⁰ However, already during the reaction the formation of disulfide was observed. Attempts to reduce this disulfide to the corresponding thiol were incomplete (Tris(2-carboxyethyl)-phosphine (TCEP)^{71,72} or NaBH₄) or oxidation during workup or in the NMR tube (which was not a case for **2a** and **2b**) took place. Therefore, in the case of **2c** all tests with proteins were performed with the corresponding disulfide.

Experimental Design and Surface Grafting with Monothiolated Glycerol Dendrons. The grafting of the gold surface was performed by the chemisorption of monothiolated glycerol dendrons with different sizes and functionalities, which were synthesized for the examination of our hypothesis (Figure 1). Gold substrates were precleaned by immersion in piranha solution for 30 s and subsequent washing steps in Milli-Q water and ethanol. All chemisorption experiments were carried out by immersion of the gold chip in an 1 mM ethanolic solution of an adequate thiol at room temp, which was diluted from a 10 mM stock solution kept in dark. Fresh precleaned gold chips were immersed into the thiol solution for 0.5, 2, 4, 6, and 24 h, followed by rinsing with EtOH for 30 s, and dried under a stream of argon.

SPR spectroscopy has been applied for a quantitative evaluation of protein adsorption on the modified surfaces from the aqueous solution as a reliable detection system. Exposure of

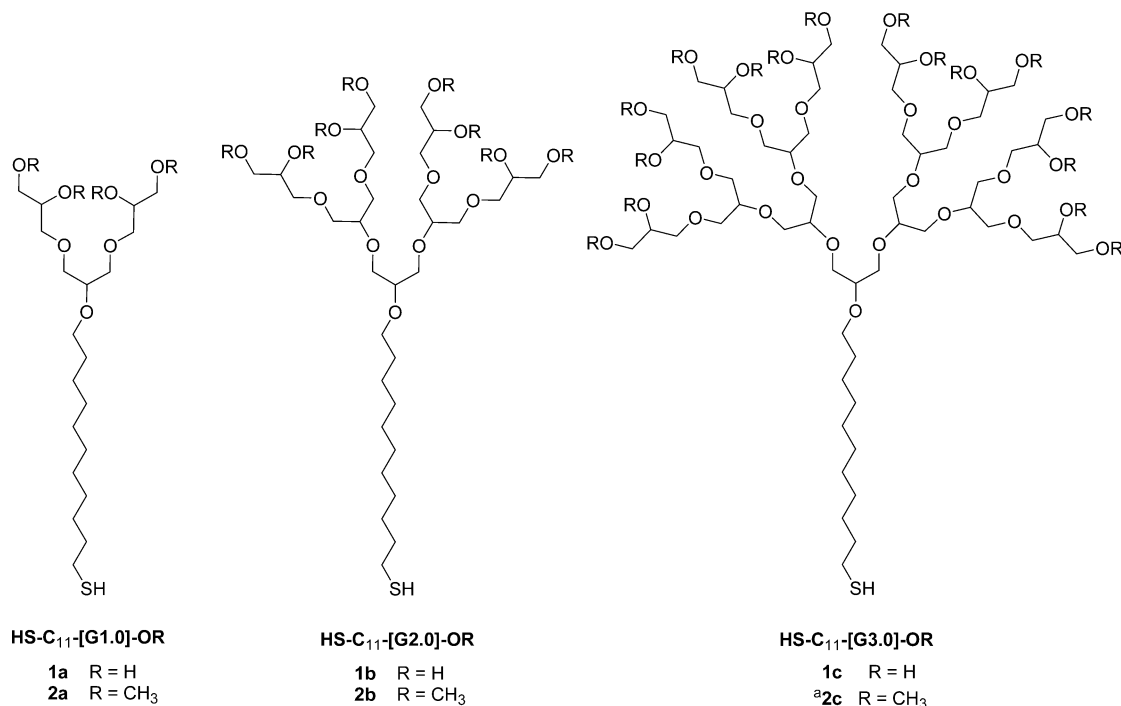


Figure 1. Chemical structures of alkanethiol polyglycerol dendrons derivatives used in protein resistance study. ^aCompound **2c** was only obtained as a disulfide.

Table 1. Time-Dependent Fibrinogen (Fib) Adsorption on Dendritic SAMs **1a–c**^a

time [h]	dendron					
	[G1.0]-OH (1a)		[G2.0]-OH (1b)		[G3.0]-OH (1c)	
	ΔRU	% PA	ΔRU	% PA	ΔRU	% PA
0.5	21.1 ± 9.5	0.5 ± 0.3	220.0 ± 80.4	5.0 ± 2.3	209.3 ± 96.8	4.8 ± 2.8
2.0	13.6 ± 3.2	0.3 ± 0.1	342.9 ± 76.5	7.8 ± 2.2	24.3 ± 13.7	0.6 ± 0.4
4.0	6.4 ± 2.5	0.1 ± 0.1	86.8 ± 23.9	2.0 ± 0.7	217.5 ± 27.5	4.9 ± 0.8
6.0	20.3 ± 6.8	0.5 ± 0.2	379.7 ± 103.3	8.6 ± 3.0	249.5 ± 54.3	5.7 ± 1.6
24.0	0.3 ± 2.0	0.0 ± 0.1	342.9 ± 101.4	7.8 ± 2.9	499.4 ± 136.4	11.4 ± 3.9

^a HDT was used as a reference surface, $\Delta RU = 4398.6$; PA = 100%.

each modified surface to protein solutions in the flow cells of the SPR spectrometer allows us to determine the amount of adsorbed proteins. The amount of protein absorbed (ΔRU = change in refractive units) as measured by SPR was determined by subtracting the value of RU before and after the exposure to the protein solution ($\Delta RU_{PG} = RU_{10 \text{ min after exposure}} - RU_{\text{before exposure}}$). As a reference, we used a very hydrophobic surface such as HDT (n-hexadecanethiol), upon which a monolayer of protein adsorbs ($\Delta RU_{HDT} = 100\%$). Thus, the relative amount of adsorbed proteins (% PA) could be calculated from the following equation:

$$\%PA = \frac{\Delta RU_{PG}}{\Delta RU_{HDT}} \times 100$$

The ΔRU values of 2–4 protein-adsorption measurements for the same modified surface were used to calculate the standard deviation, which was further used to estimate the error in relative adsorption (% PA) by using the mean square method.

Study of Protein Adsorption using Dendritic Polyglycerol Alkanethiol Derivatives. Our previous study on protein adsorption after surface modification with hyperbranched polyglycerols (hPG) derivatives conjugated with thiotic acid demonstrate excellent protein resistant properties.²⁴ Furthermore, a structure–activity relationship was designed to investigate the

reasons hiding behind these results.⁵⁰ The effects of the dendrons generation and the surface functionalization (OH vs OMe) with polyglycerol dendrons on protein adsorption were studied. A general decrease of nonspecific protein adsorption with an increasing molecular weight of the glycerol dendrons, with minimum adsorption level obtained for [G2.0], was observed. However, the applied method for the coupling of the amino polyglycerol derivatives onto the anhydride functionalized surfaces implicate unexpected problems.⁵⁰ Therefore, a series of glycerol dendrons self-assembled monolayers were prepared to study their nonfouling properties.

a. Study of Fibrinogen Adsorption on Hydrophilic SAMs. Besides such factors like packing density,^{33,73–75} length,^{21,76} order and conformation of PEG chains,^{36,77} and variation of surface coverage changes the level of adsorbed proteins.⁷⁸ Vanderah et al showed dependency of the protein adsorption on coverage of gold surface with PEG-thiolate and obtained minimum adsorption levels at ~55–80% surface coverage. Based on these results and our own observations,⁵⁰ we varied the density of the surface monolayer of compounds **1** and **2a–c** by exposing a gold substrate for different immersion times. Table 1 and Figure 2 present the results obtained by the screening of the SAMs of [G1.0]–[G3.0]-OH (**1a–c**) with Fib as test protein.

Gold surfaces modified with [G1.0]-OH thiolate (**1a**) showed a dramatic decrease of the Fib adsorption on the SAMs.

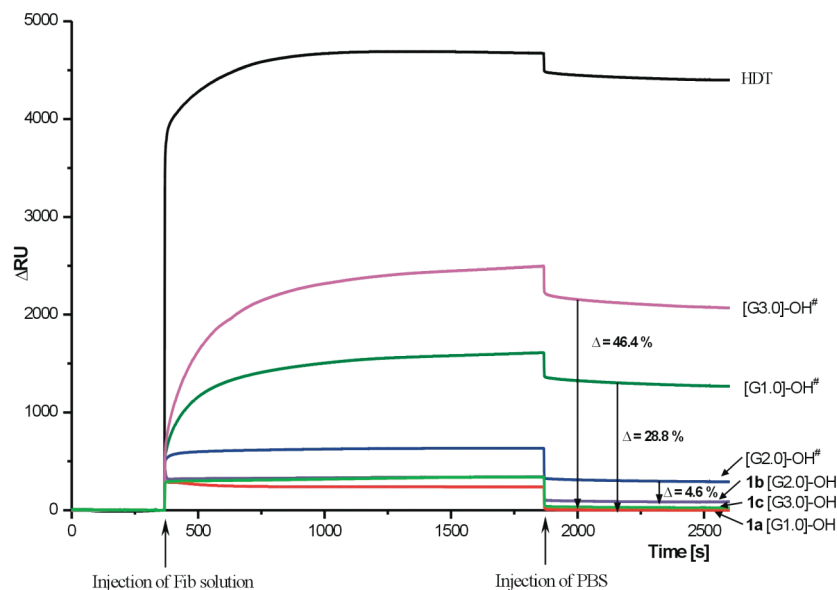


Figure 2. Surface plasmon resonance sensograms of fibrinogen adsorption on SAMs formed by alkanethiols of polyglycerol dendrons [Gn]-OH (1a–c) compared to the SAMs obtained by functionalization of the surface by coupling of monoamino dendrons [Gn]-OH[#] to the anhydride.

Table 2. Time-Dependent Fibrinogen (Fib) Adsorption on Dendritic SAMs 2a–c^a

time [h]	dendron					
	[G1.0]-OMe (2a)		[G2.0]-OMe (2b)		[G3.0]-OMe (2c)	
	ΔRU	% PA	ΔRU	% PA	ΔRU	% PA
0.5	64.3 ± 7.1	1.5 ± 0.2	61.9 ± 3.5	1.4 ± 0.1	65.4 ± 39.5	1.5 ± 0.9
2.0	1260 ± 223.9	28.6 ± 6.4 ^b	130.3 ± 7.3	3.0 ± 0.2	52.3 ± 35.2	1.2 ± 1.0
4.0	91.9 ± 10.6	2.1 ± 0.3	1695.7 ± 199.5	38.6 ± 5.7 ^b	185.4 ± 70.3	4.2 ± 2.0
6.0	107.7 ± 14.1	2.4 ± 0.4	75.5 ± 7.2	1.7 ± 0.2	69.7 ± 28.0	1.6 ± 0.8
24.0	103.7 ± 10.5	2.4 ± 0.3	26.3 ± 3.5	0.6 ± 0.1	29.9 ± 14.3	0.7 ± 0.4

^a HDT was used as a reference surface, ΔRU = 4398.6; PA = 100%. ^b High values are probably a result of poor chip quality.

However, only after 30 min monolayer formation we did not observe significant changes in the amount of adsorbed proteins within the studied time frame of 24 h (detailed data shown in the Table 1). It is also surprising that the simple, small, and easily accessible [G1.0] dendron derivative exhibits the same inertness as previously studied hyperbranched polyglycerol (with $M_n = 5000$ g/mol). Similar, albeit a little bit higher protein adsorption values than [G1.0]-OH SAMs were obtained for SAMs of higher dendrimer generation, which was about 5% higher. Nevertheless, very low levels of adsorption were as well detected for **1b** and **1c** SAMs (2.0 and 0.6%, respectively). In contrast to the results obtained by surface modification with polyglycerol monoamines (reaction of amino group with a reactive anhydride on the surface)^{49,69} and the one presented by Adronov et al.⁵³ (dendronization of PEG with bis-MPA), no clear tendency in the inertness against proteins of the different generations was observed.

Figure 2 compares the results from the screening with Fib of the surfaces modified with polyglycerol dendrons [G1.0]–[G3.0] obtained via both functionalization methods, namely, by the coupling of amine to an anhydride⁵⁰ and by chemisorption of the alkanethiols. Obviously, elimination of low coupling efficiency of the amino group of the dendrons by synthesis of the alkanethiols led to the significant improvements of the protein resistant properties of the dendrons grafted to the surface and confirms our previous hypothesis.

b. Study of Fibrinogen Adsorption on Hydrophobic SAMs. The effect of surface modification with polyglycerol dendrons with methylated terminal groups on protein adsorption was investigated as well. When analyzing data from the SPR

screening with Fib on methylated surfaces, it became apparent that the amount of the adsorbed Fib is almost invariable, regardless of dendrimer generation (Table 2). Observed high values in case of [G1.0]-OMe and [G2.0]-OMe are probably a result of poor chip quality. In this case, as well as for the nonmethylated SAMs, detected changes of the amount of adsorbed proteins with increasing exposition time are very small. Figure 3 presents the results from the screening with Fib obtained on both surfaces prepared by the “anhydride method” and by chemisorption. The protein adsorption was reduced by 5–10% as compared to compounds **1a–c**, which confirmed again our previous hypothesis.

c. Study of Lysozyme, Albumin, and Pepsin Adsorption on Dendritic SAMs. To determine whether the degree of adsorption is influenced by the nature of protein, we chose much smaller proteins Lys, Alb, and Pep as compared to Fib. Tables 3 and 4 present the results obtained by the screening of the SAMs of [G1.0]–[G3.0] polyglycerol dendrons (**1** and **2**) with those proteins. For all these proteins we did not observe time and generation dependency. However, methylated compounds in contrast to the nonmethylated show a slightly higher adsorption. Positively charged Lys gives higher adsorption values of [G2.0] and [G3.0] SAMs than negatively charged Pep; however, in the case of [G1.0], these values are similar for both proteins. This might suggest that other factors that the overall charge of the proteins under experiment conditions take place. When compared the size of these proteins, Lys (14 kDa) with pepsin (34 kDa), this could explain why Lys adsorption value are higher. The small Lys could better fit into the gaps in the less-ordered monolayer than in the case of [G1.0]. Globular and

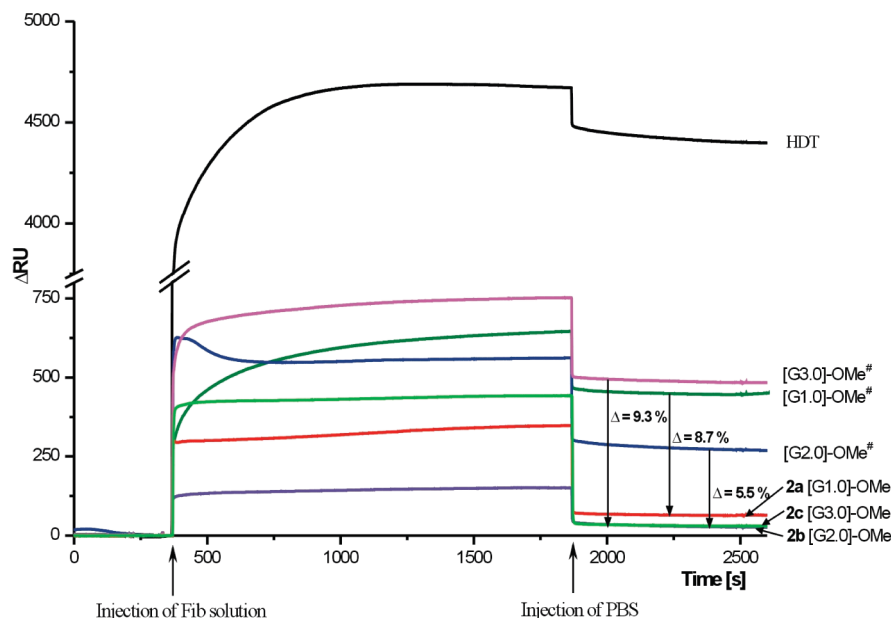


Figure 3. Surface plasmon resonance sensograms of fibrinogen adsorption on SAMs formed by alkanethiols of polyglycerol dendrons [Gn]-OMe (2a–c) compared to the SAMs obtained by functionalization of the surface by coupling of monoamino dendrons [Gn]-OMe[#] to the anhydride. For clarity the scale up to 750 ΔRU was amplified.

Table 3. Time-Dependent Lysozyme, Albumin, and Pepsin Adsorption on Dendritic SAMs 1a–c^a

dendron	[G1.0]-OH (1a)			[G2.0]-OH (1b)			[G3.0]-OH (1c)		
time [h]	Lys ^b	Alb ^c	Pep ^d	Lys ^b	Alb ^c	Pep ^d	Lys ^b	Alb ^c	Pep ^d
0.5	0.1 ± 0.1	−0.4 ± 0.2	0.9 ± 0.1	4.6 ± 2.7	1.5 ± 0.1	−0.6 ± 0.3	5.3 ± 1.6	5.9 ± 1.7	4.4 ± 0.1
2.0	−0.1 ± 0.1	−0.7 ± 0.3	2.3 ± 0.4	2.4 ± 0.8	1.5 ± 0.2	1.1 ± 0.3	0.2 ± 0.1	0.4 ± 0.1	0.3 ± 0.1
4.0	−0.2 ± 0.1	−1.0 ± 0.3	2.2 ± 0.8	3.0 ± 2.0	0.9 ± 0.3	0.8 ± 0.4	6.1 ± 0.8	2.6 ± 0.7	0.7 ± 0.3
6.0	0.8 ± 0.2	0.1 ± 0.1	0.1 ± 0.1	8.1 ± 3.4	1.8 ± 0.1	1.1 ± 0.1	4.8 ± 1.3	1.4 ± 0.2	0.6 ± 0.4
24.0	−0.6 ± 0.2	−0.8 ± 0.3	1.3 ± 0.4	23.9 ± 3.4 ^e	1.5 ± 0.2	7.8 ± 0.6 ^e	9.9 ± 3.8	1.6 ± 0.3	0.5 ± 0.1

^a HDT was used as a reference surface, PA = 100%. ^b ΔRU = 1194.1. ^c ΔRU = 1325.2. ^d ΔRU = 1785.4. ^e High values are probably a result of poor chip quality.

Table 4. Time-Dependent Lysozyme, Albumin, and Pepsin Adsorption on Dendritic SAMs 2a–c^a

dendron	[G1.0]-OMe (2a)			[G2.0]-OMe (2b)			[G3.0]-OMe (2c)		
time [h]	Lys ^b	Alb ^c	Pep ^d	Lys ^b	Alb ^c	Pep ^d	Lys ^b	Alb ^c	Pep ^d
0.5	2.7 ± 0.7	0.1 ± 0.1	1.5 ± 0.2	2.9 ± 0.2	0.5 ± 0.1	−0.2 ± 0.1	2.9 ± 0.2	4.9 ± 0.2	1.3 ± 0.1
2.0	15.4 ± 3.4 ^e	22.8 ± 3.7 ^e	6.4 ± 0.8	9.4 ± 0.07	4.4 ± 0.2	0.8 ± 0.2	9.9 ± 3.3 ^e	3.9 ± 0.1	0.9 ± 0.1
4.0	1.0 ± 0.2	1.0 ± 0.1	0.3 ± 0.1	21.9 ± 3.5 ^e	25.9 ± 5.4 ^e	5.6 ± 1.7	6.7 ± 0.3	6.1 ± 0.3	5.4 ± 2.0
6.0	1.6 ± 0.4	0.3 ± 0.1	0.7 ± 0.1	1.3 ± 0.1	0.5 ± 0.1	−0.3 ± 0.1	6.4 ± 0.8	5.3 ± 0.2	3.1 ± 0.5
24.0	3.3 ± 0.2	0.8 ± 0.2	0.6 ± 0.1	4.4 ± 0.2	0.0 ± 0.1	−0.6 ± 0.2	2.2 ± 0.1	2.3 ± 0.1	0.4 ± 0.1

^a HDT was used as a reference surface, PA = 100%. ^b ΔRU = 1194.1. ^c ΔRU = 1325.2. ^d ΔRU = 1785.4. ^e High values are probably a result of poor chip quality.

bigger than Lys and Pep, albumin gave low values of % PA for all tested polyglycerol alkanethiol surfaces. Again, it is obvious that the SAMs based on the smallest oligomers **1a** gives extremely high resistance toward all tested proteins.

Water Contact Angle Measurements. The water contact angle was measured for each immersion time for all polyglycerol dendron derivatives. For an immersion time longer than 0.5 h for [G1.0]-OH and after 2 h for [G2.0]- and [G3.0]-OH the obtained water contact angle achieved $20 \pm 2^\circ$, as measured previously for hPG.²⁴ For methylated compounds, the CA was higher as detected before,^{24,50} namely, $56 \pm 2^\circ$, and does not depend on the dendrimer size and exhibition time. Based on these results we can definitely say that the inertness of a surface is not correlated with hydrophilicity (−OH) or hydrophobicity (−OMe) of these materials, and the reason for previously observed dependency was connected with poor coupling efficiency. In addition, the values of the water contact angle measured for all surfaces ($\sim 20^\circ$ and $\sim 56^\circ$ for −OH and −OMe,

respectively) may suggest that the main part of the monolayer formation seems to take place at times shorter than 30 min for [G1.0]-OH and 2 h for [G2.0]- and [G3.0]-OH.

Monolayer Formation. X-ray Photoelectron Spectroscopy Results. XPS spectra of [G1.0] polyglycerol dendron monolayers formed on gold by deposition in ethanolic solution for 0.5 and 2 h are shown in Figure 4. The carbon 1s region of the spectra (Figure 4b) for polyglycerol dendrons monolayer can be deconvoluted into two peaks, one at 285.1 eV for the alkyl chain and at 286.0 eV assigned to the etheric carbon present in the polyglycerol dendrons. The oxygen region of the spectrum (Figure 4c) shows mainly one peak, centered at 535.3 eV, assigned to the etheric oxygen, indicative of the presence of polyglycerol. The second, small signal at ~ 530.5 eV can be attributed to carbon contamination.⁷⁹ The XPS spectrum of the S 2p region (Figure 4a) with BE at 162.3 eV assigned to the S–Au bound at low coverage of thiol SAMs on Au.⁸⁰ The deconvolution of a S 2p_{3/2}/S 2p_{1/2} region shows two peaks, with

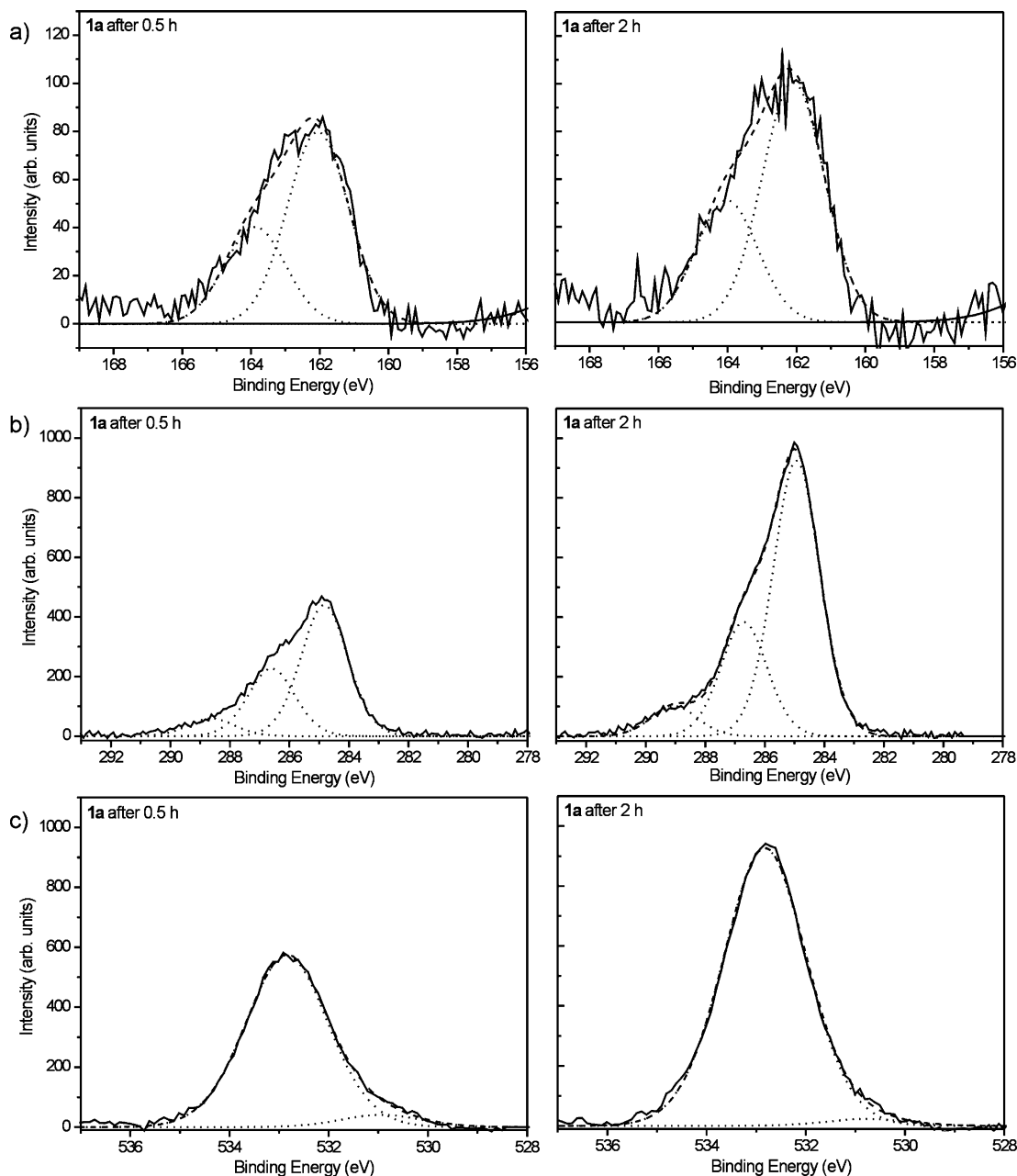


Figure 4. XPS spectra of HS-C₁₁-[G1.0]-OH after 0.5 h (left column) and 2 h immobilization (right column) for (a) sulfur 2p, (b) carbon 1s, and (c) oxygen 1s regions. Experimental data are plotted in solid lines, fitted spectra in dashed lines, and fits for each component in dotted lines.

an intensity ratio of about 2:1 with BEs of ≈ 162.1 eV for (S 2p_{3/2}) and ≈ 163.8 eV for S 2p_{1/2}, which is typical for an alkyl-thiolate species bounded to the gold surface.^{81,82}

We observe a significant signal growth over time in all relevant regions (S 2p, C 1s, and O 1s) of the XP spectra indicating increase of the packing density of the SAMs on the gold surface. To prove that, the surface coverage and lateral packing density has been determined according to the previously described procedure in literature.^{33,36,83} Namely, it has been shown that attenuation length of the metal substrate photoelectrons (Au 4f) decrease exponentially with increasing adsorbate thickness. Therefore, we use series of three unsubstituted alkanethiols (C₁₁–C₁₈) with 11, 16, and 18 carbon atoms as a reference to determine the relative thickness of the oligoglycerol terminated self-assembled monolayers (Figure 5). As an example, the Au 4f signal intensity of the dendron monolayers was inserted into the

calibration diagram (Figure 5, red diamonds) and the approximately average thickness of the glycerol dendron monolayer of **1a** after 0.5 and 2 h immobilization were obtained. The experimental data show that the attenuation of the Au 4f by a HS-C₁₁-[G1.0]-OH (**1a**) film with 20 carbon atoms and 7 oxygen atoms after 0.5 h and after 2 h immobilization is identical to the attenuation obtained by an unsubstituted alkanethiol film on gold with ~ 14.3 and ~ 17.5 of carbon atoms on average, respectively. This implies that the relative coverage of **1a** increase with an immobilization time from 53 to 65% (using a value of 1.26 Å per methylene unit).³⁶

Summary and Conclusions

Here we described a simple approach for the synthesis of alkanethiols based on polyglycerol dendrons with different

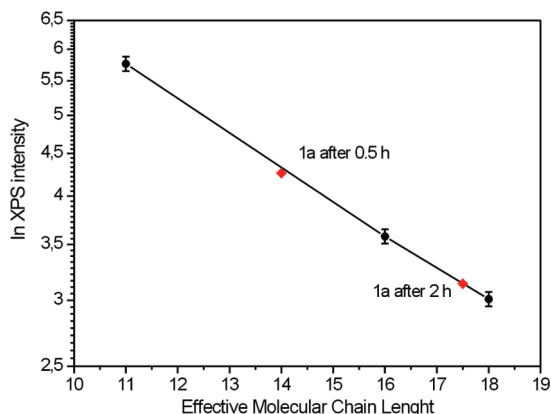


Figure 5. Attenuation of the substrate photoelectron intensity for alkanethiol SAMs with 11, 16, and 18 carbon atoms and 100% surface coverage. The logarithmic Au 4f intensities decrease linearly with increasing molecular chain length of unsubstituted alkanethiols and can be used as a reference to determine the effective thickness of glycerol dendrons SAMs.

functionalities on the dendritic terminal groups. These dendritic polyglycerol derivatives were used to study their resistance against proteins by direct adsorption on gold. The monolayer formation was confirmed by XPS analysis. A structure–activity relationship of the polymer architecture forming the self-assembled monolayers has been revealed by SPR measurements, with detection of the adsorption of four model proteins as well as contact-angle measurements of water droplets. In contrast to a previously used screening approach, the synthesis of defined polyglycerol-alkane thiols overcomes problems and complications of heterogeneous surface. For these reasons we used direct chemisorption of the thiols to the gold surface.

Although very little is known for the protein resistance of dendritic structures on surfaces in literature, we can conclude from our experiments the following:

In contrast to previous findings, we observe by direct chemisorption the highest protein resistance for the smallest dendron **1a**. This might be due to the ability of **1a** to form a better and more defined monolayer. In the case of higher generations, the monolayer became less defined, and therefore, small proteins like Lys or Pep can penetrate the monolayer. Significant improvement of protein adsorption for the alkane thiols based dendrons as compared to the adsorption values recently obtained for polyglycerol dendrons coupled to the carboxylic anhydride, proved our presumption that formation of the hydrogen bonding with carboxylic acid group and poor accessibility of the amino group in the core of the dendron might reduce the coupling efficiency of the dendrons and, hence, increase the protein adsorption.

Elimination of the hydrogen-donor groups by methylation does not have any more of an influence on the nonfouling properties of the monolayer. That would suggest the previously observed dramatic effect of methylation was strongly connected with difficult conditions of the coupling of the nonmethylated dendrons.

This structure–property study clearly shows that dendritic polyglycerol oligomers are an excellent alternative to the PEGylated surfaces. Already a [G1.0] oligoglycerol dendron (MW: 426 g mol⁻¹) is highly protein resistant (<0.5% PA). Additionally, presence of multiple free -OH groups, beside their high resistance to nonspecific protein adsorption, gives the possibility to further functionalization with ligands for specific interactions. Thus, use of the polyglycerol as a background

instead of common dextrane layer^{24,84} would allow the minimization/avoidance of the nonspecific interactions at the same time.

For the practical applications, in the future we will concentrate on the study of the monolayer formation by the polyglycerol thiol derivatives under different conditions by control of ionic strength, concentration of the thiol solution and by using other techniques than SPR.

Acknowledgment. The authors are thankful for the generous gifts of Dr. W. Dilla (Solvay Chemicals GmbH, triglycerol) and Dr. U. Bierfreund (Biacore, SIA Kit) as well as for help and support concerning the SPR measurements. Authors are grateful to Dr. C. Navio and A. Krüger for XPS measurements, analysis, and intensive discussions during writing of this manuscript. W. Münch, M. Selent, and K. Biskup are acknowledged for synthesis and HPLC separation of the dendrons. The authors thank the Deutsche Forschungsgemeinschaft (SFB 658) for financial support.

References and Notes

- (1) Ratner, B. D.; Hoffman, A. S.; Schoen, F. J.; Lemons, J. E. *Biomaterials Science. An Introduction to Materials in Medicine*; Academic Press: New York, NY, 1996.
- (2) Dee, K. C.; Puleo, D. A.; Bizios, R. *An Introduction to Tissue–Biomaterial Interactions*; John Wiley & Sons, Inc.: Hoboken, NJ, 2002.
- (3) *Service Characteristics of Biomedical Materials and Implants*; Batchelor, A. W., Chandrasekaran, M., Eds.; Imperial College Press: London, 2004; Vol. 3.
- (4) Anderson, J. M.; Rodriguez, A.; Changb, D. T. *Semin. Immunol.* **2008**, *20*, 86–100.
- (5) Castner, D. G.; Ratner, B. D. *Surf. Sci.* **2002**, *500*, 28–60.
- (6) Ratner, B. D.; Bryant, S. J. *Annu. Rev. Biomed. Eng.* **2004**, *6*, 41–75.
- (7) Krishnan, S.; Weinman, C. J.; Ober, C. K. *J. Mater. Chem.* **2008**, *18*, 3405–3413.
- (8) Frazier, R. A.; Matthijs, G.; Davies, M. C.; Roberts, C. J.; Schacht, E.; Tendler, S. J. B. *Biomaterials* **2000**, *21*, 957–966.
- (9) Salzman, E.; Merrill, E.; Binder, A.; Wolf, C. F. W.; Ashford, T. P.; Austen, W. G. *J. Biomed. Mater. Res.* **1969**, *3*, 69–81.
- (10) De Sousa Delgado, A.; Léonard, M.; Dellacherie, E. *Langmuir* **2001**, *17*, 4386–4391.
- (11) Morra, M.; Cassinelli, C. J. *Biomater. Sci., Polym. Ed.* **1999**, *10*, 1107–1124.
- (12) Luk, Y.-Y.; Kato, M.; Mrksich, M. *Langmuir* **2000**, *16*, 9604–9608.
- (13) Metzke, M.; Bai, J. Z.; Guan, Z. *J. Am. Chem. Soc.* **2003**, *125*, 7760–7761.
- (14) Metzke, M.; Guan, Z. *Biomacromolecules* **2008**, *9*, 208–215.
- (15) Urakami, H.; Guan, Z. *Biomacromolecules* **2008**, *9*, 592–597.
- (16) Konradi, R.; Pidhatika, B.; Muehlebach, A.; Textor, M. *Langmuir* **2008**, *24*, 613–616.
- (17) Ladd, J.; Zhang, Z.; Chen, S.; Hower, J. C.; Jiang, S. *Biomacromolecules* **2008**, *9*, 1357–1361.
- (18) Chang, Y.; Liao, S.-C.; Higuchi, A.; Ruaan, R.-C.; Chu, C.-W.; Chen, W.-Y. *Langmuir* **2008**, *24*, 5453–5458.
- (19) Chen, S.; Zheng, J.; Li, L.; Jiang, S. *J. Am. Chem. Soc.* **2005**, *127*, 14473–14478.
- (20) Pale-Grosdemange, C.; Simon, E. S.; Prime, K. L.; Whitesides, G. M. *J. Am. Chem. Soc.* **1991**, *113*, 12–20.
- (21) Prime, K. L.; Whitesides, G. M. *J. Am. Chem. Soc.* **1993**, *115*, 10714–10721.
- (22) Wang, R. L. C.; Kreuzer, H. J.; Grunze, M. *J. Phys. Chem. B* **1997**, *101*, 9767–9773.
- (23) Heyes, C.; D.; Groll, J.; Möller, M.; Nienhaus, G. U. *Mol. Biosyst.* **2007**, *3*, 419–430.
- (24) Siegers, C.; Biesalski, M.; Haag, R. *Chem.–Eur. J.* **2004**, *10*, 2831–2838.
- (25) Gordienok, N. I.; Freidin, B. G.; Proskurina, L. S. *Zh. Prikl. Khim.* **1986**, *59*, 1549–1554.
- (26) Herold, D. A.; Keil, K.; Bruns, D. E. *Biochem. Pharmacol.* **1989**, *38*, 73–76.
- (27) Talarico, T.; Swank, A.; Privalle, C. *Biochem. Biophys. Res. Commun.* **1998**, *250*, 354–358.
- (28) Sadana, A. *Chem. Rev.* **1992**, *92*, 1799–1818.
- (29) Andrade, J. D.; Hlady, V. *Adv. Polym. Sci.* **1986**, *79*, 1–63.

- (30) Chapman, R. G.; Ostuni, E.; Takayama, S.; Holmlin, R. E.; Yan, L.; Whitesides, G. M. *J. Am. Chem. Soc.* **2000**, *122*, 8303–8304.
- (31) Ostuni, E.; Chapman, R. G.; Holmlin, R. E.; Takayama, S.; Whitesides, G. M. *Langmuir* **2001**, *17*, 5605–5620.
- (32) Holmlin, R. E.; Chen, X.; Chapman, R. G.; Takayama, S.; Whitesides, G. M. *Langmuir* **2001**, *17*, 2841–2850.
- (33) Herrwerth, S.; Eck, W.; Reinhardt, S.; Grunze, M. *J. Am. Chem. Soc.* **2003**, *125*, 9359–9366.
- (34) Morra, M. J. *Biomater. Sci., Polym. Ed.* **2000**, *11*, 547–569.
- (35) Latour, R. A. *J. Biomed. Mater. Res., Part A* **2006**, *78A*, 843–854.
- (36) Harder, P.; Grunze, M.; Dahint, R.; Whitesides, G. M.; Laibinis, P. E. *J. Phys. Chem. B* **1998**, *102*, 426–436.
- (37) Jeon, S. I.; Andrade, J. D. *J. Colloid Interface Sci.* **1991**, *142*, 159–165.
- (38) Jeon, S. I.; Lee, J. H.; Andrade, J. D.; De Gennes, P. G. *J. Colloid Interface Sci.* **1991**, *142*, 149–158.
- (39) Szleifer, I. *Curr. Opin. Solid State Mater. Sci.* **1997**, *2*, 337–344.
- (40) Szleifer, I. *Curr. Opin. Colloid Interface Sci.* **1996**, *1*, 416–423.
- (41) Fang, F.; Szleifer, I. *Biophys. J.* **2001**, *80*, 2568–2589.
- (42) Fang, F.; Satulovsky, J.; Szleifer, I. *Biophys. J.* **2005**, *89*, 1516–1533.
- (43) Chapman, R. G.; Ostuni, E.; Liang, M. N.; Meluleni, G.; Kim, E.; Yan, L.; Pier, G.; Warren, H. S.; Whitesides, G. M. *Langmuir* **2001**, *17*, 1225–1233.
- (44) Frey, H.; Haag, R. *Rev. Mol. Biotechnol.* **2002**, *90*, 257–267.
- (45) Kainthan, R. K.; Janzen, J.; Levin, E.; Devine, D. V.; Brooks, D. E. *Biomacromolecules* **2006**, *7*, 703–709.
- (46) Kainthan, R. K.; Janzen, J.; Kizhakkedathu, J. N.; Devine, D. V.; Brooks, D. E. *Biomaterials* **2008**, *29*, 1693–1704.
- (47) Kainthan, R. K.; Gnanamani, M.; Ganguli, M.; Ghosh, T.; Brooks, D. E.; Maiti, S.; Kizhakkedathu, J. N. *Biomaterials* **2006**, *27*, 5377–5390.
- (48) Kainthan, R. K.; Brooks, D. E. *Biomaterials* **2007**, *28*, 4779–4787.
- (49) Wyszogrodzka, M.; Haag, R. *Polym. Prepr. (Am. Chem. Soc., Div. Polym. Chem.)* **2007**, *48*, 760–761.
- (50) Wyszogrodzka, M.; Haag, R. *Langmuir* **2009**, in press.
- (51) Yan, L.; Marzolin, C.; Terfort, A.; Whitesides, G. M. *Langmuir* **1997**, *13*, 6704–6712.
- (52) Ostuni, E.; Chapman, R. G.; Liang, M. N.; Meluleni, G.; Pier, G.; Ingber, D. E.; Whitesides, G. M. *Langmuir* **2001**, *17*, 6336–6343.
- (53) Benhabbour, S. R.; Liu, L.; Sheardown, H.; Adronov, A. *Macromolecules* **2008**, *41*, 2567–2576.
- (54) Ulman, A. *Chem. Rev.* **1996**, *96*, 1533–1554.
- (55) Love, J. C.; Estroff, L. A.; Kriebel, J. K.; Nuzzo, R. G.; Whitesides, G. M. *Chem. Rev.* **2005**, *105*, 1103–1169.
- (56) Ostuni, E.; Yan, L.; Whitesides, G. M. *Colloids Surf., B* **1999**, *15*, 3–30.
- (57) Schreiber, F. *J. Phys.: Condens. Matter* **2004**, *16*, R881–R900.
- (58) Vericat, C.; Vela, M. E.; Benitez, G. A.; Gago, J. A. M.; Torrelles, X.; Salvarezza, R. C. *J. Phys.: Condens. Matter* **2006**, *18*, R867–R900.
- (59) Schreiber, F. *Prog. Surf. Sci.* **2000**, *65*, 151–256.
- (60) Senaratne, W.; Andruzzi, L.; Ober, C. K. *Biomacromolecules* **2005**, *6*, 2427–2448.
- (61) Delamarche, E.; Michel, B.; Biebuyck, H. A.; Gerber, C. *Adv. Mater.* **1996**, *8*, 719–729.
- (62) Chechik, V.; Crooks, R. M.; Stirling, C. J. M. *Adv. Mater.* **2000**, *12*, 1161–1171.
- (63) Green, R. J.; Frazier, R. A.; Shakesheff, K. M.; Davies, M. C.; Roberts, C. J.; Tendler, S. J. B. *Biomaterials* **2000**, *21*, 1823–1835.
- (64) Homola, J. *Chem. Rev.* **2008**, *108*, 462–493.
- (65) Schaller, J.; Gerber, S.; Kämpfer, U.; Lejon, S.; Trachsel, C. *Human Blood Plasma Proteins: Structure and Function*; John Wiley & Sons, Ltd.: Chichester, England, 2008.
- (66) Hahn, C. D.; Tinazli, A.; Hoelzl, M.; Leitner, C.; Frederix, F.; Lackner, B.; Mueller, N.; Klampfl, C.; Tampe, R.; Gruber, H. J. *Monatsh. Chem.* **2007**, *138*, 245–252.
- (67) According to the manufactured instruction (BIAcore), the gold chips should only be cleaned by sonication in pure ethanol; however, it was shown (see ref 66) that this method is not sufficient. Despite boiling of the gold chip in SC1 solution giving good results, we decide to use piranha solution for cleaning, mainly due to safety reasons.
- (68) Wyszogrodzka, M.; Haag, R. *Chem.—Eur. J.* **2008**, *14*, 9202–9214.
- (69) Wyszogrodzka, M.; Möws, K.; Kamlage, S.; Wodzinska, J.; Plietker, B.; Haag, R. *Eur. J. Org. Chem.* **2008**, *5*, 3–63.
- (70) Svedhem, S.; Hollander, C.-A.; Shi, J.; Konradsson, P.; Liedberg, B.; Svensson, S. C. T. *J. Org. Chem.* **2001**, *66*, 4494–4503.
- (71) Burns, J. A.; Butler, J. C.; Moran, J.; Whitesides, G. M. *J. Org. Chem.* **1991**, *56*, 2648–2650.
- (72) Cline, D. J.; Redding, S. E.; Brohawn, S. G.; Psathas, J. N.; Schneider, J. P.; Thorpe, C. *Biochemistry* **2004**, *43*, 15195–15203.
- (73) Malmsten, M.; Emoto, K.; Van Alstine, J. M. *J. Colloid Interface Sci.* **1998**, *202*, 507–517.
- (74) Unsworth, L. D.; Sheardown, H.; Brash, J. L. *Langmuir* **2008**, *24*, 1924–1929.
- (75) Unsworth, L. D.; Sheardown, H.; Brash, J. L. *Langmuir* **2005**, *21*, 1036–1041.
- (76) Yang, Z.; Galloway, J. A.; Yu, H. *Langmuir* **1999**, *15*, 8405–8411.
- (77) Vanderah, D. J.; Valincius, G.; Meuse, C. W. *Langmuir* **2002**, *18*, 4674–4680.
- (78) Vanderah, D. J.; La, H.; Naff, J.; Silin, V.; Robinson, K. A. *J. Am. Chem. Soc.* **2004**, *126*, 13639–13641.
- (79) Lilley, C. M.; Huang, Q. *Appl. Phys. Lett.* **2006**, *89*, 203114/1–203114/3.
- (80) Rodriguez, J. A.; Dvorak, J.; Jirsak, T.; Liu, G.; Hrbek, J.; Aray, Y.; Gonzalez, C. *J. Am. Chem. Soc.* **2003**, *125*, 276–285.
- (81) Frey, S.; Stadler, V.; Heister, K.; Eck, W.; Zharnikov, M.; Grunze, M.; Zeysing, B.; Terfort, A. *Langmuir* **2001**, *17*, 2408–2415.
- (82) Tielens, F.; Costa, D.; Humblot, V.; Pradier, C.-M. *J. Phys. Chem. C* **2008**, *112*, 182–190.
- (83) Laibinis, P. E.; Bain, C. D.; Whitesides, G. M. *J. Phys. Chem.* **1991**, *95*, 70717–7021.
- (84) Dextran thin layer is commonly used as a background in biochips (e.g., CM-5 chip from BIAcore).

BM801093T